

# Calculation of the Effects of Branching and Conjugation on Intrinsic Barriers for H Atom Transfer Reactions Involving Hydrocarbons

Donald M. Camaioni,\* S. Tom Autrey, Terrance B. Salinas, and James A. Franz

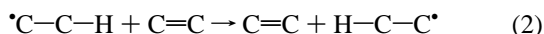
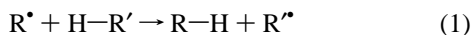
Contribution from the Pacific Northwest National Laboratory, Box 999,  
Richland, Washington 99352-0999

Received March 6, 1995<sup>⊗</sup>

**Abstract:** This paper describes the use of the semiempirical molecular orbital (MO) theoretical methods (AM1 and MNDO-PM3) to calculate barriers for a series of H atom transfer reactions involving alkyl, alkenyl, arylalkyl, and hydroaryl systems. Transition state (TS) energies were calculated for a series of known H abstractions and show to correlate linearly with experimental TS energies. Barriers for H abstraction reactions decrease with the degree of alkyl substitution at the radical site, and increase with the degree of conjugation. Barriers for transfer of a  $\beta$ -hydrogen from a radical to an unsaturated hydrocarbon (radical hydrogen transfer or RHT) were also calculated. The results show that methyl group substitutions at the radical site lower the barrier while substitutions at the site  $\beta$  to the radical, the position from which the H originates, raise the barrier. The barriers for RHT reactions involving conjugated systems increase with increasing radical delocalization and correlate linearly with the strength of the donor radical  $\beta$ -C–H bond. RHT barriers are estimated to range from  $E_a \approx 17$ –20 kcal/mol for benzene-plus-cyclohexadiene to  $E_a \approx 26$ –29 kcal/mol for anthracene-plus-9-hydroanthracene.

## Introduction

Hydrogen transfer reactions play a well-recognized role in many thermal and catalytic processes involving the production of fuels and chemicals. While H abstraction reactions (eq 1) between radicals and H donors have been well studied, the understanding of structure–reactivity relationships remains surprisingly incomplete. Another form of hydrogen transfer (eq 2) known as radical hydrogen transfer (RHT)<sup>1–5</sup> is currently the subject of much speculation.



RHT is unusual in that the radical donates a  $\beta$ -hydrogen to an acceptor molecule rather than abstracting hydrogen from a donor molecule. RHT is known to take place readily between ketones and ketyl radicals.<sup>6</sup> But in hydrocarbon systems, it remains controversial due to a lack of information about its activation barrier. The reaction is thought to be important in high-temperature liquid-phase reactions of hydrocarbons<sup>2,3c</sup> and

in coal liquefaction<sup>3c,4</sup> where it provides a simple route for migration of hydrogen from hydroaryl to aryl structures and for cleavage of aryl–alkyl bonds. However, multistep reaction pathways to the same products are usually possible. For RHT to be important, its activation barrier must be sufficiently low to compete with these alternative pathways. In particular, RHT must compete with unimolecular scission of a H atom from the radical and subsequent rapid reactions of free H atoms. A recent ab initio calculation of the RHT reaction of ethyl plus ethylene (eq 2) obtained a barrier of 27.2 kcal/mol.<sup>7</sup> For comparison, the energy for ethyl radical to dissociate to ethylene and a H atom is 36 kcal/mol (see below). Although the RHT reaction barrier is substantially less, the RHT reaction still may not compete because the Arrhenius *A* factors for unimolecular scissions are  $\sim 10^6$  times larger than typical *A* factors for bimolecular H transfer reactions.<sup>4,8</sup> Therefore, the importance of RHT reactions in condensed phase reactions, such as coal liquefaction, depends on how this barrier changes on going to higher homologs and analogs such as cyclic hydroaryl/arene systems.

The Bell–Evans–Polanyi relationship<sup>9</sup> expressed by eq 3 is used routinely to correlate and predict rates of H abstraction by hydrocarbon radicals. The constant *C*, which corresponds to the

$$E_a = \alpha \Delta H_r + C \quad (3)$$

activation barrier if the reaction were to occur with zero enthalpy change, is the intrinsic barrier. It is assumed to be constant for

<sup>⊗</sup> Abstract published in *Advance ACS Abstracts*, February 1, 1996.

(1) Jackson, R. A.; Waters, W. A. *J. Chem. Soc.* **1958**, 4632.

(2) Metzger, J. O. *Angew. Chem., Int. Ed. Engl.* **1986**, 25, 80.

(3) (a) Billmers, R.; Griffith, L. L.; Stein, S. E. *J. Phys. Chem.* **1986**,

90, 517. (b) Billmers, R.; Brown, R. L.; Stein, S. E. *Int. J. Chem. Soc.*

**1989**, 21, 375. (c) Stein, S. E. *Acc. Chem. Res.* **1991**, 24, 350.

(4) (a) Malhotra, R.; McMillen, D. F. *Energy Fuels* **1993**, 7, 227. (b)

McMillen, D. F.; Malhotra, R.; Tse, D. S. *Energy Fuels* **1991**, 5, 179. (c)

Malhotra, R. and McMillen, D. F. *Energy Fuels* **1990**, 4, 184. (d) McMillen,

D. F.; Malhotra, R.; Hu, G. P.; Chang, S.-J. *Energy Fuels* **1987**, 1, 193. (e)

McMillen, D. F.; Malhotra, R.; Chang, S.-J.; Ogier, W. C.; Nigenda, S. E. *Fuels* **1987**, 66, 1611.

(5) Savage, P. E. *Energy Fuels* **1995**, 9, 590–598.

(6) (a) Wagner, P. J.; Zhang, Y.; Puchalski, A. E. *J. Phys. Chem.* **1993**,

97, 13368. (b) Naguib, Y. M. A.; Steel, C.; Cohen, S. G. *J. Phys. Chem.*

**1988**, 92, 6574–6579. (c) Malwitz, D.; Metzger, J. O. *Angew. Chem., Int.*

*Ed. Engl.* **1986**, 25, 762–763; *Chem. Ber.* **1986**, 119, 3558–3575. (d)

Schuster, D. I.; Karp, P. B. *J. Photochem.* **1980**, 12, 333–344. (e) Neckers,

D. C.; Schaap, A. P.; Harry, J. *J. Am. Chem. Soc.* **1966**, 88, 1265.

(7) The cited value is for a PMP2/6-31G\*\* calculation that includes corrections for spin annihilation and thermal and zero-point energy differences. Franz, J. A.; Ferris, K. F.; Camaioni, D. M.; Autrey, S. T. *Energy Fuels* **1994**, 8, 1016.

(8) Mallard, W. G.; Westley, F.; Herron, J. T.; Hampson, R. F. *NIST Chemical Kinetic Database-Ver. 6.0*; NIST Standard Reference Data: Gaithersburg, MD, 1994.

(9) Bell, R. P. *Proc. R. Soc. London* **1936**, A154, 414. Evans, M. G.; Polanyi, M. *Trans. Faraday Soc.* **1936**, 32, 1333.

structurally related reactants, but according to Marcus theory,<sup>10,11</sup> the intrinsic barrier for a nonidentity reaction is approximately the average of that for the two contributing identity reactions. Unfortunately, barriers for only a small number of identity reactions have been measured. Lack of knowledge about how barriers for identity reactions differ for hydrocarbon systems limit one's ability to estimate rate constants accurately using eq 3. This paper uses calculations to determine how *C* may depend on structure.

Molecular orbital (MO) theory-based calculations provide powerful tools for gaining fundamental understanding of how molecular structures of radicals and H donors may control H abstraction reaction rates. Theoretical studies<sup>10,12,13</sup> of H abstraction reactions of simple hydrocarbons and functionalized methanes have shown significant variation in intrinsic barrier heights. However, the understanding of structural effects is still incomplete: although these studies have shown how the effects of alkyl and heteroatom functional groups attached to the reaction site affect the intrinsic barrier, the effects of delocalizing groups such as vinyl and aryl groups on intrinsic barriers for H abstraction remain to be examined. Aromatic systems are dominant structures in coal, and hydroaromatic and aromatic hydrocarbons are key components in hydroliquefaction solvents. Understanding their reactivity is necessary to understanding and advancing coal liquefaction processes. Because no kinetic data are available for hydrocarbon RHT reactions, theory-based insights to rate-controlling factors are needed to aid experimental verification and elucidation of this pathway.

We report MO calculations of the effects of both alkyl structure and conjugation on intrinsic barriers for hydrocarbon H abstraction and radical hydrogen transfer reactions using both the AM1<sup>14</sup> and the PM3<sup>15</sup> parameterizations of the minimum neglect of differential overlap (MNDO) formalism. A previous theoretical study of hydrocarbon H abstraction reactions by Dannenberg and Lluch<sup>16</sup> using AM1 found that intrinsic barriers for methyl radical H abstractions increase with the degree of branching in the H donor. This finding differs markedly from *ab initio*<sup>12</sup> and experimental results<sup>8,17</sup> which indicate that intrinsic barriers decrease as branching increases. We attribute the failure of the method to noncanceling errors in calculated energies for reactants and transition states. The AM1 Hamiltonian yields energies that correlate linearly with experimental values, although slopes and intercepts differ according to structural types.<sup>18</sup> This characteristic causes the accuracy of calculated reaction enthalpies and activation energies to be dependent on the types and sizes of structures calculated. Recently, Beckwith and Zavitsas<sup>19</sup> have reported that AM1 calculations of dioxolanes, compounds related to dioxolanes, and radicals derived from these compounds were highly consistent with experimental data. Much of their success, as well as that of others cited therein,<sup>18</sup> may be due to the fact that their calculations were limited to a select class of

compounds and radicals. Stewart<sup>15</sup> has shown that, in comparison to AM1, MNDO-PM3 gives overall smaller average deviations from experimental energies. Yet, deviations from experimental values are still significant (see below), such that consistent results may not be obtained without compensating for the various systematic errors inherent in the method. In the following sections, we describe our approach to mitigating the problem of noncanceling errors, present our findings regarding the effects of alkyl structure and conjugation on H transfer reactions, and discuss their implications regarding the radical hydrogen transfer reaction in hydrocarbon systems.

## Computational Methodology

MNDO-PM3 and AM1 calculations of geometries and energies ( $\Delta H_f^\circ$ ) were performed using MOPAC (Quantum Chemistry Program Exchange, Department of Chemistry, Indiana University, Bloomington, IN; QCPE No. 455, version 6.0). Geometries of transition states for H atom transfer reactions were optimized using the default RHF Hamiltonian which includes Dewar's<sup>20</sup> half-electron correction for odd-electron systems. Transition states (TSs) for identity reactions were located using either the default optimizer or the eigen following optimizer (in which case, the EF and precise keywords were also specified) while forcing the breaking/forming C–H bonds to have equal lengths using symmetry. TS geometries for nonidentity reactions were optimized using one or more of the following methods available in MOPAC, version 6: Bartel's nonlinear least squares minimization routine, the McIver–Komornicki gradient minimization routine, and the eigenvector follower (TS and precise keywords) optimizers. In our hands, the eigen follower optimizers (TS and EF keywords) were superior methods for optimizing polycyclic systems. Force calculations were performed to establish that optimized geometries actually were saddle points for H transfer (only one negative vibrational frequency).

The  $\Delta H_f^\circ$  for radicals and donors were obtained from the literature<sup>21–28</sup> or derived from standard estimation methods (see Lias et al.<sup>21</sup>). Rate data for H abstraction reactions are from the literature.<sup>17,29</sup> For reactions in which temperature-dependent rate data are lacking, Arrhenius activation energies ( $E_{a,r}$ ) were estimated using eq 4, which equates the

$$E_{a,2} - E_{a,1} = n_1/n_2 \ln(k_2/k_1) \quad (4)$$

(20) Dewar, M. J. S.; Hashmall, J. A.; Venier, C. G. *J. Am. Chem. Soc.* **1968**, *90*, 1953.

(21) Lias, S. G.; Bartmess, J. E.; Liebman, J. F.; Holmes, J. L.; Levin, R. D.; Mallard, W. G. *J. Phys. Chem. Ref. Data* **1988**, *17*, Suppl 1.

(22) Cox, J. D.; Pilcher, G. *Thermochemistry of Organic and Organometallic Compounds*; Academic Press: New York, 1970; p 516.

(23) (a) Griller, D.; Simões, J. A. M.; Sim, B. A.; Wayner, D. D. M. *J. Am. Chem. Soc.* **1989**, *111*, 7872. (b) Clark, K. B.; Culshaw, P. N.; Griller, D.; Lossing, F. P.; Simões, J. A. M.; Walton, J. C. *J. Org. Chem.* **1991**, *56*, 5535–5539.

(24) Seakins, P. W.; Pilling, M. J.; Niiranen, J. T.; Gutman, D.; Krasnoperov, L. N. *J. Phys. Chem.* **1992**, *96*, 9847.

(25) Tsang, W. *J. Phys. Chem.* **1984**, *88*, 2812.

(26) Tsang, W. *J. Phys. Chem.* **1986**, *90*, 1152.

(27) Bordwell, F. G.; Cheng, J.-P.; Harrelson, J. A., Jr. *J. Am. Chem. Soc.* **1988**, *110*, 1229–1231.

(28) McMillen, D. F.; Trevor, P. L.; Golden, D. M. *J. Am. Chem. Soc.* **1980**, *102*, 7400–7402. This work determined the  $\Delta H_f^\circ$  values of 1-naphthylmethyl and 9-anthrylmethyl radicals by measuring the BDEs of 1-ethylnaphthalene and 9-ethylanthracene and assigning the  $\Delta H_f^\circ$  values of 1-ethylnaphthalene and 9-ethylanthracene using group additivity methods. Recalculation of the value for the 9-anthrylmethyl radical gives 76 kcal/mol instead of 79.9 as reported. We estimated the  $\Delta H_f^\circ$ (9-ethylanthracene) by correcting the PM3 value (50.0 kcal/mol) downward by 5.7 kcal/mol, the difference between the PM3 (61.7 kcal/mol) and experimental (55 kcal/mol) values for anthracene.<sup>21</sup> Accordingly, the BDE for 9-methylanthracene is 80 kcal/mol using  $\Delta H_f^\circ$ (9-methylanthracene) = 48 kcal/mol.<sup>21</sup> Correcting the PM3 value (54.3 kcal/mol) for 9-methylanthracene downward by 5.7 kcal/mol gives  $\Delta H_f^\circ$  = 48.6 kcal/mol.

(29) (a) Bockrath, B.; Bittner, E.; McGrew, J. *J. Am. Chem. Soc.* **1984**, *106*, 135. (b) Franz, J. A.; Alnajjar, M. S.; Barrows, R. D.; Kaisaki, D. L.; Camaioni, D. M.; Suleman, N. K. *J. Org. Chem.* **1986**, *51*, 1446. (c) Jackson, R. A.; O'Neill, D. W. *J. Chem. Soc. D* **1969**, 1210–1211. (d) Manka, M. J.; Brown, R. L.; Stein, S. E. *Int. J. Chem. Kinet.* **1987**, *19*, 943.

(10) Marcus, R. A. *J. Phys. Chem.* **1968**, *72*, 891.

(11) Fox, G. L.; Schlegel, H. B. *J. Phys. Chem. Soc.* **1992**, *96*, 298–302.

(12) Yamataka, H.; Nagase, S. *J. Org. Chem.* **1988**, *53*, 3232.

(13) Pross, A.; Yamataka, H.; Nagase, S. *J. Phys. Org. Chem.* **1991**, *4*, 135.

(14) Dewar, M. J. S.; Zoebisch, E. G.; Healy, E. F.; Stewart, J. J. P. *J. Am. Chem. Soc.* **1985**, *107*, 3902.

(15) Stewart, J. J. P. *J. Comput. Chem.* **1989**, *10*, 209, 221.

(16) Lluch, J. M.; Bertran, J.; Dannenberg, J. J. *Tetrahedron* **1988**, *44*, 7621–7625. Dannenberg, J. J. *Adv. Mol. Model.* **1990**, *2*, 1.

(17) Kerr, J. A. In *Free Radicals*; Kochi, J. K., Ed.; Wiley, New York: 1973; Vol. 1, p 15.

(18) (a) Camaioni, D. M. *J. Am. Chem. Soc.* **1991**, *112*, 9475. (b) Kass, S. R. *J. Comput. Chem.* **1990**, *11*, 94–104.

(19) Beckwith, A. L. J.; Zavitsas, A. A. *J. Am. Chem. Soc.* **1995**, *117*, 607–614.

difference in activation energies between the reaction of interest and a basis reaction of known activation energy with the log of the relative rate constant at a known temperature, and statistically corrected for the number of donatable hydrogens. Because reactions of methyl and ethyl radicals reacting with primary, secondary, tertiary, and allylic C–H show significant curvature in their Arrhenius plots,  $E_a$  were determined from eq 4 using rate constants<sup>8</sup> at 300 K and the  $E_a$ <sup>8</sup> for reaction of methyl plus methane.

Users of AM1 or PM3 must heed a general warning for reaction enthalpy and barrier calculations: *failure to correct or account for errors in the energies of various species involved can lead to erroneous trends because combined errors may not cancel or even be constant.*

## Results

### Analysis of Errors in the AM1 and MNDO-PM3 Methods.

This portion of the results section shows that PM3 calculations exhibit trends similar to those of AM1 and that recognition of this fact allows one to considerably improve agreement with experimental energies.

Herndon et al.<sup>30</sup> have collected experimental  $\Delta H_f^\circ$  for 11 polycyclic benzenoid aromatic hydrocarbons<sup>31</sup> and evaluated the abilities of various empirical and semiempirical methods including AM1 to reproduce the values. In the case of AM1, the average error is 9 kcal/mol. By comparison, other methods including PCMODEL,<sup>32</sup> MM3,<sup>33</sup> and group additivity schemes all had average errors under 2 kcal/mol. However, using Herndon's data, we find that the linear correlation for experimental  $\Delta H_f^\circ$  vs AM1 calculated values is quite good ( $r^2 = 0.988$ ), yielding a slope of 0.849 and intercept of 1.108. Using the regression parameters to estimate  $\Delta H_f^\circ$  from the AM1 values leads to an average error of only 1.3 kcal/mol.

We also used PM3 to calculate the  $\Delta H_f^\circ$  of the same 11 compounds.<sup>34</sup> While the average error at 5.86 kcal/mol is somewhat less than that for AM1, the linear correlation with  $r^2 = 0.973$  is not as good. Figure 1 shows the least squares fit to both the AM1 and PM3 values for Herndon compounds. The resulting average error for  $\Delta H_f^\circ$  estimates using the PM3 regression parameters (slope 0.942, intercept 2.15) is 2.05 kcal/mol. Interestingly, if least squares fitting is limited to compounds for which  $\Delta H_f^\circ$  are known most accurately, i.e., benzene, naphthalene, phenanthrene, and anthracene, then excellent correlations are obtained ( $r^2 = 0.99951$  for AM1 and 0.99992 for PM3). Furthermore, using these regression parameters to make estimates for the whole group leads to average errors of 1.2 kcal/mol for AM1 and 2.1 kcal/mol for PM3 that are equivalent to those obtained above from fits to the whole data set.

Analogous trends are expected for other classes of closed shell molecules, as well as for open shell molecules and transition structures. Figure 2 plots PM3 calculated  $\Delta H_f^\circ$  for hydrocarbon free radicals vs experimental  $\Delta H_f^\circ$ .<sup>35</sup> The figure shows that while considerable scatter exists for the radicals taken as a whole, the errors are systematic for families of structurally-related radicals. For example, primary, secondary, and tertiary radicals each exhibit an excellent correlation, deviating  $-12$ ,

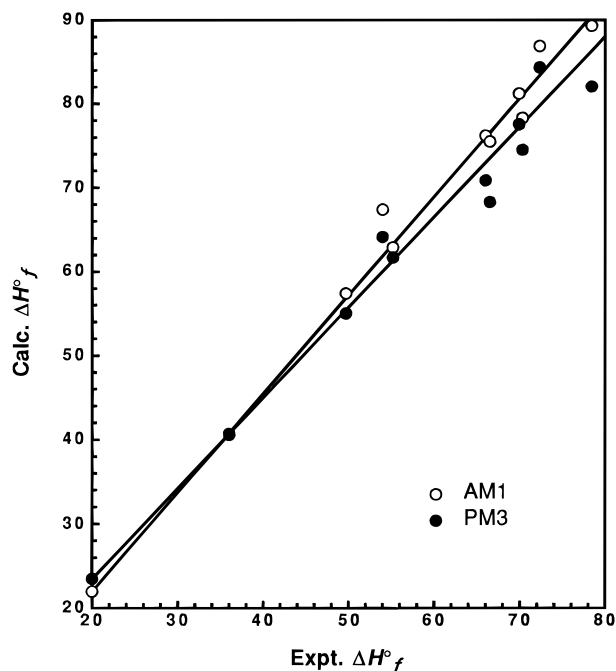


**Figure 1.** PM3 (●)<sup>34</sup> and AM1 (○)<sup>30</sup> calculated  $\Delta H_f^\circ$  values for polycyclic benzenoid aromatic hydrocarbons correlate linearly with experimental values.<sup>30</sup>

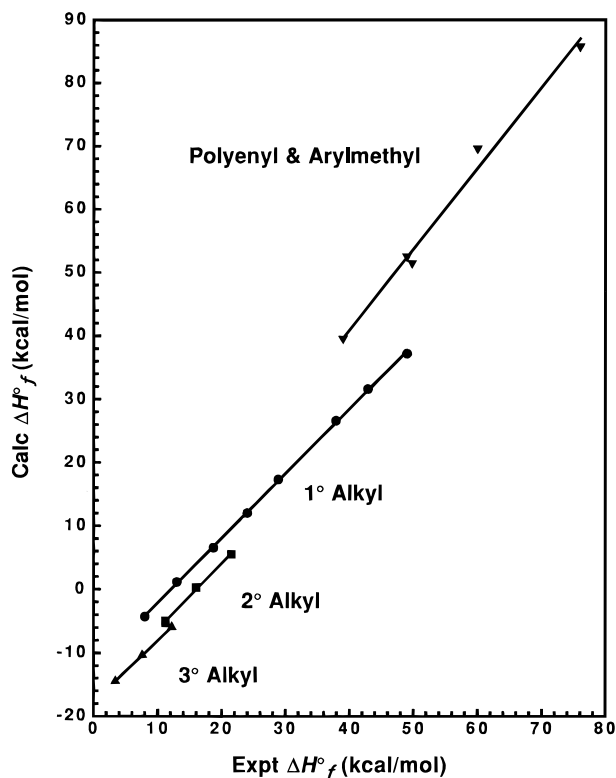


**Figure 2.** Graph of PM3  $\Delta H_f^\circ$  vs experimental  $\Delta H_f^\circ$  for radicals:<sup>35</sup> although considerable scatter exists for radicals taken as a whole, errors are systematic for families of structurally related radicals.

$-16$ , and  $-18$  kcal/mol, respectively, from experiment. Allylic and benzylic radicals, for which group homologation effects are nonadditive, exhibit nonunit slopes.

Table 1 lists calculated and experimental TS energies for 22 different H abstraction reactions. As shown in Figure 3, PM3 energies for H atom transfer TSs correlate with experimental TS energies. The experimental values were obtained by summing the activation enthalpy and  $\Delta H_f^\circ$  for the abstracting radical and hydrogen donor molecule for each reaction (eq 5).

(30) Herndon, W. C.; Nowak, P. C.; Connor, D. A.; Lin, P. *J. Am. Chem. Soc.* **1992**, *114*, 41–47.

(31) Benzene, naphthalene, anthracene, phenanthrene, tetracene, benz[a]anthracene, chrysene, triphenylene, benzo[c]phenanthrene, pyrene, and perylene.

(32) PCMODEL, Version 3, Serena Software, Box 3076, Bloomington, IN. Gajewski, J. J.; Gilbert, K. E.; McKelvey, J. *Adv. Mol. Model.* **1990**, *2*, 65.

(33) Allinger, N.; Li, F.; Tai, J. C. *J. Comput. Chem.* **1990**, *11*, 868.

(34) The  $\Delta H_f^\circ$  (kcal/mol) values calculated for the compounds using PM3: benzene, 23.5; naphthalene, 40.7; phenanthrene, 55; anthracene, 61.7; pyrene, 64.1; triphenylene, 68.3; chrysene, 70.9; benz[a]anthracene, 74.5; benzo[c]phenanthrene, 77.6; perylene, 82; tetracene, 84.3.

**Table 1.** Calculated and Experimental TS Energies for H Abstraction Reactions

no.	transition state (R–H–R') <sup>‡</sup>	E <sub>a</sub> <sup>a</sup>	ΔH <sub>f</sub> <sup>o</sup> (reactant) <sup>b</sup>		ΔH <sub>f</sub> <sup>o</sup> (TS) (R–HR') <sup>c</sup>			TS bond distances <sup>d</sup>	
			R•	H–R'	exptl	PM3	AM1	C–H <sup>‡</sup>	C'–H <sup>‡</sup>
1	Et, <i>t</i> -Bu	10.0	28.85	-32.1	6.2	-2.6	4.56	1.381	1.300
2	Me, <i>t</i> -Bu	8.3	34.8	-32.1	10.4	7.2		1.415	1.253
3	Et, <i>i</i> -Pr	11.4	28.85	-25.	14.8	4.9		1.34	1.307
4	Me, <i>s</i> -Bu	10.0	34.8	-30.2	14.0	9.16		1.384	1.249
5	Me, <i>n</i> -Bu	11.5	34.8	-30.2	15.6	10.4		1.330	1.257
6	Me, <i>i</i> -Pr	9.3	34.8	-25.	18.5	14.1		1.385	1.248
7	Et, Et	13.3	28.85	-20.1	21.5	12.7		1.308	1.308
8	Me, Et	11.5	34.8	-20.1	25.7	21.1		1.338	1.252
9	Me, Me	14.6	34.8	-17.8	31.0	28.5	38	1.275	1.275
10	Me, 2-methyl-3-butenyl	7.3	34.8	-6.5	35.0	33.8		1.419	1.251
11	Me, cumyl	7.8	34.8	1	43.0	43.5		1.424	1.257
12	Me, allyl	9.8	34.8	4.8	48.8	14.1	52.8	1.331	1.257
13	Me, benzyl	9.5	34.8	12	55.7	55.3	62.3	1.338	1.263
14	benzyl, 1,2,3,4-tetrahydronaphthalene	13.2	49	6	67.5	65.51		1.371	1.314
15	benzyl, ethylbenzene	14.5	49	7	69.8	71.46		1.372	1.312
16	benzyl, benzyl	15.8	49	12	76.2	78.7	83	1.325	1.325
17	benzyl, 9-hydroanthryl	9.6	49	38.2	96.2	99.0		1.393	1.308
18	benzyl, 9-hydrophenanthryl	11.9	49	36.6	96.9	99.8		1.371	1.319
19	benzyl, fluorenyl	10.6	49	45	104	112.1	125	1.338	1.334
20	benzyl, diphenylmethyl	12.8	49	37.3	98.5	105.4		1.356	1.347
21	diphenylmethyl, diphenylmethyl	18	67.9	37.3	121.9	132.4		1.365	1.365
22	benzyl, triphenylmethane	11	49	65	124.5	136.1	144	1.378	1.352

<sup>a</sup> Activation energies (kcal/mol) from experimental kinetic data: entries 1–9 and 12, ref 8; entries 10, 11, and 13, ref 57; entry 17, ref 29b; entries 17–19, ref 29a,b; entry 20, ref 29d; entries 21 and 22, ref 29a. <sup>b</sup> Experimental ΔH<sub>f</sub><sup>o</sup> (kcal/mol): methyl and benzyl, ref 21; ethyl, ref 24; diphenylmethyl, ref 27; donors, ref 21, except for entry 17 and 18, ref 58. <sup>c</sup> The TS value is the MNDO-PM3 ΔH<sub>f</sub><sup>o</sup> value obtained for the TS structure with the listed C–H<sup>‡</sup> and C'–H<sup>‡</sup> distances. <sup>d</sup> Bond distance (Å) between inflight H atoms and terminal C atoms at the TS.

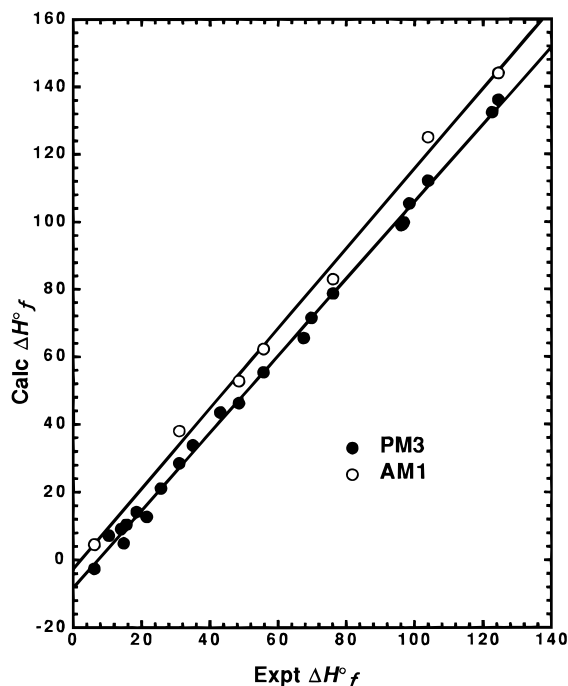


**Figure 3.** PM3 (●) and AM1 (○) ΔH<sub>f</sub><sup>o</sup> values for H abstraction transition states correlate linearly with experimental heats (data from Table 1). Reaction enthalpies for these H abstraction reactions range from thermoneutral to -20 kcal/mol. Note that intercepts are <0 and slopes are <1.

$$\Delta H_f^o(\text{TS}) = E_a - RT + \Delta H_f^o(\text{R-H}) + \Delta H_f^o(\text{R}^\bullet) \quad (5)$$

The linear correlation (see Figure 3) between the measured and PM3 TS enthalpies is surprisingly good ( $r^2 = 0.9978$ , standard error ΔH<sub>f</sub><sup>o</sup> = 2.2 kcal/mol), especially considering that the data base includes reactions of methyl, ethyl, benzyl, and diphenylmethyl radicals with alkane, alkene, and aromatic donors and reaction enthalpies ranging from thermoneutral to -20 kcal/mol. Equation 6 provides the linear regression equation that

$$\Delta H_{f,\text{calcd}}(\text{TS}) = 1.143\Delta H_{f,\text{exptl}}(\text{TS}) - 8.256 \text{ kcal/mol} \quad (6)$$

relates MNDO-PM3 TS energies to measured TS energies. Unlike the correlation for alkyl radicals, a simple offset correction will not suffice to reproduce experimental data. Depending on the magnitude of the TS energy, calculated TS energies can be smaller than, equal to, or greater than experimental energies.

Several of the TS energies were calculated using the AM1 Hamiltonian and are included in the table for comparison to PM3. Notably, the AM1 correlation (AM1 vs experiment), although based on a smaller data set, has a slope of 1.185 and intercept of -2.650 such that, for these TSs, the AM1 values are greater than the corresponding PM3 values, and this difference increases with increasing TS energy.

The above findings indicate that both minima and maxima on AM1 or PM3 potential energy surfaces for H transfer correlate with experiment. With this insight, consistent structure-barrier trends may be obtained for H transfer reactions provided that the necessary corrections are applied.<sup>36</sup> We have opted to use mainly experimental data for reactants in the barrier

(35) The data for Figure 2 are as follows (kcal/mol) (radical, exptl, PM3): hexyl, 8, -4.3; pentyl, 13, 1.1; butyl, 18.7, 6.6; propyl, 24, 12; ethyl, 28.9, 17.3; 5-hexenyl, 37.9, 26.6; 4-pentenyl, 42.9, 31.6; butenyl, 49, 37.2; isopropyl, 21.5, 5.5; *sec*-butyl, 16.0, 2; 2-pentyl, 11.2, -5.2; 3-pentyl, 11.2, -5.0; *tert*-butyl, 12.2, -5.9; *tert*-pentyl, 7.6, -10.4; 3-methyl-3-pentyl, 3.4, -14.5; allyl, 41.7,<sup>25</sup> 39.6; pentadienyl, 49.8,<sup>23b</sup> 51.5; benzyl, 49,<sup>21</sup> 52.6; 1-naphthylmethyl, 59.6,<sup>28</sup> 69.6; 9-anthrylmethyl, 76,<sup>28</sup> 85.8. Experimental ΔH<sub>f</sub><sup>o</sup> values of alkyl radicals were derived from BDEs and ΔH<sub>f</sub><sup>o</sup> values for actual or homologous compounds (*i.e.*, ΔH<sub>f</sub><sup>o</sup> values for primary, secondary, and tertiary radicals obtained from BDEs for the C–H of ethane,<sup>24</sup> secondary C–H of propane,<sup>24</sup> and tertiary C–H of isobutane<sup>24</sup> and ΔH<sub>f</sub><sup>o</sup> values of precursor hydrocarbons<sup>21</sup>).

(36) A reviewer points out that eq 6 probably will not be generally applicable for correcting H transfer TS energies. We have noted that methylene homologations of hydrocarbons and alkyl radicals give correlations (calculated vs experimental) with unit slope (see Figure 2), whereas homologations with interacting groups, *i.e.*, vinyl or benzo homologations, lead to nonunit slopes (see Figure 1, and benzylic and allylic radicals in Figure 2). Accordingly, if an E<sub>a</sub> for a H abstraction reaction is desired for a system that can be obtained by homologating one of the systems in Table 1 with noninteracting groups, then the E<sub>a</sub> of that base system should be used.

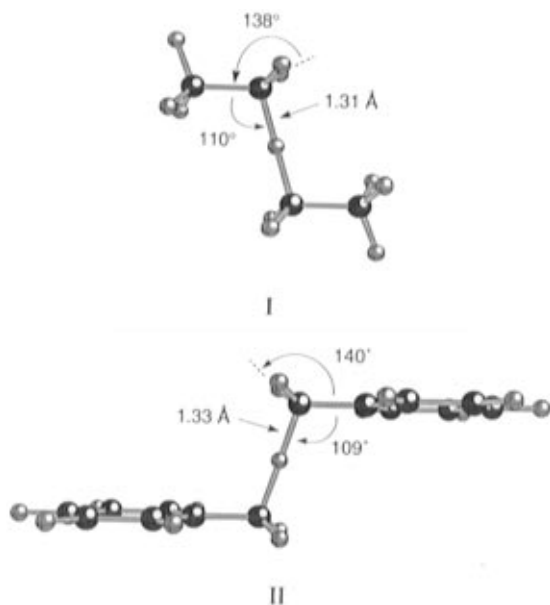
**Table 2.** Bond Orders and Geometric Parameters for Reaction Site Carbons in H Transfer Transition Structures and Reactants<sup>a</sup>

structure	p- $\sigma$	p- $\pi$	$\angle(\text{H}^\ddagger-\text{C}-\text{C})$ (deg)	C...H <sup>†</sup> (Å)
ethyl (radical site carbon)	2.0	0.11	110.6 <sup>b</sup>	1.098 <sup>b</sup>
benzyl (radical site carbon)	2.0	0.53		
cyclohexadienyl (methylene carbon)	2.85	0.14	109.2	1.111
9-hydroanthryl (methylene carbon)	2.9	0.11	108.9	1.111
ethane	3.0	0	111.6	1.098
toluene (methyl carbon)	3.0	0	110.8	1.098
methyl-plus-methane TS	2.57		105.9	1.275
ethyl-plus-ethane TS	2.54	0.05	110.4	1.308
isopropyl-plus-propane TS	2.52	0.08	107.4	1.340
tert-butyl-plus-isobutane TS	2.51	0.11	104.8	1.370
benzyl-plus-toluene TS	2.52	0.15	109.2	1.325
ethyl-plus-ethylene TS	2.42	0.57	105.4	1.420
2-butenyl-plus-butadiene TS	2.45	0.53	107.1	1.401
2,4-hexadienyl-plus-1,3,5-hexatriene TS	2.46	0.52	107.5	1.401
cyclohexadienyl-plus-benzene TS	2.38	0.60	102.9	1.469
1-hydronaphthyl-plus-naphthalene TS	2.40	0.58	103.3	1.453
9-hydroanthracene-plus-anthracene TS	2.43	0.55	103.9	1.441

<sup>a</sup> All carbons have s- $\sigma$ -bond orders of 1; p- $\sigma$ -bond orders are 2 for sp<sup>2</sup> carbons and 3 for sp<sup>3</sup> carbons; p- $\pi$ -bond order is 2 for pure olefinic and aromatic carbons. <sup>b</sup> Entries are parameters for the methyl group in the ethyl radical.

calculations that we present below, because it reduces the number of structures that have to be calculated and eliminates the need to correct for reactant errors. In the rest of this paper, we examine how barriers for H transfer identity reactions correlate with reactant and TS properties. Results for H abstraction reactions are discussed first followed by RHT reactions.

**Transition Structures for H Abstraction Reactions.** The TS structures calculated for ethyl-plus-ethane (I) and benzyl-plus-toluene (II) reactions are depicted below. Like these



structures, the TS structures calculated for other H abstraction reactions generally have linear three-centered C-H-C bonds with pyramidal C atoms intermediate between sp<sup>2</sup> and sp<sup>3</sup> geometries. For TSs involving delocalized radicals such as structure II, overlap of the atomic orbitals (AO) of the breaking/forming C-H bond with adjacent  $\pi$ -delocalized orbitals is less than that in the reactant radical. Quantitative evidence for this condition is provided in Table 2, which lists  $\sigma$ - $\pi$ -bond orders (calculated using the MOPAC "pi" keyword) for representative molecules, radicals, and TSs. The p- $\sigma$  and p- $\pi$  entries in Table 2 are the diagonal matrix elements of the  $\sigma$ - $\pi$ -bond order

**Table 3.** Barriers Calculated for H Abstraction Identity Reactions

R in (R-H-R) <sup>†</sup>	C-H <sup>a</sup> dist (Å)	$\Delta H^\ddagger_f$ (kcal/mol) <sup>b</sup>				
		TS	R <sup>•</sup>	H-R	$E_a^c$	$E_a^{c,d}$
methyl	1.275	29	34.8	-17.8	12.1	15.8
ethyl	1.308	13	28.9	-20.1	4.5	10.1
isopropyl	1.340	-3	21.5	-25.0	0.7	8.3
tert-butyl	1.370	-20	12.2	-32.1	0.8	10.5
benzyl	1.325	78.7	49.	12	18.3	15.7
1-naphthylmethyl	1.329	115.5	59.6 <sup>e</sup>	28 <sup>f</sup>	28.5	21.3
2-naphthylmethyl	1.326	113.6	60.2 <sup>g</sup>	27 <sup>f</sup>	27.1	20.1
9-phenanthrylmethyl	1.328	144.4	74.3 <sup>g</sup>	41 <sup>f</sup>	29.7	18.8
9-anthrylmethyl	1.338	160.3	76.0 <sup>e</sup>	48 <sup>f</sup>	36.9	24.0
allyl	1.324	62	41.7 <sup>h</sup>	4.8	16.3	15.7
1,3-pentadien-5-yl	1.329	92	49.8	18.2	24.2	20.0
1,3,5-heptatrien-7-yl	1.333	120	60 <sup>i</sup>	32	29	21.2
1,4-pentadien-3-yl	1.375	95	49.8	25.3	20.3	15.6
diphenylmethyl	1.370	12	67.9	-4.6	28.7	19.3
cyclohexadienyl	1.377	82	49.7 <sup>j</sup>	25.8	6.7	3.7
9-hydroanthryl	1.327	119	62.5 <sup>k</sup>	38.2	17.6	9.8

<sup>a</sup> Bond distance between radical/donor C and inflight H at the TS. <sup>b</sup> The TS value is the PM3 energy calculated for the TS structure found with the listed C-H distance. The radical/donor  $\Delta H^\ddagger_f$  values are values tabulated by Lias et al.<sup>21</sup> unless noted. <sup>c</sup>  $E_a = \Delta H^\ddagger_f(\text{TS}) - \Delta H^\ddagger_f(\text{reactants}) + 0.6$  kcal/mol. <sup>d</sup> Obtained by scaling the calculated TS energy using  $\Delta H^\ddagger_{f,\text{exptl}} = 0.875\Delta H^\ddagger_{f,\text{calcd}} + 7.22$  kcal/mol from eq 6. <sup>e</sup> Reference 28. <sup>f</sup> Reference 59. <sup>g</sup> Reference 60a. <sup>h</sup> Reference 25. <sup>i</sup> Reference 60b. <sup>j</sup> Reference 26. <sup>k</sup> Reference 23a.

matrix. The p- $\sigma$ -bond order represents the degree of sp hybridization at a given carbon; i.e., 2 for sp<sup>2</sup> and 3 for sp<sup>3</sup>. Values for the reaction site in H abstraction TSs are approximately 2.5, which is consistent with the pyramidal geometry of the reaction site. The p- $\pi$ -bond order represents the degree or number of  $\pi$  bonds in which the carbon atom is involved. The MNDO-PM3  $\pi$ -bond orders in the ethyl radical and the ethyl-plus-ethane TS are both zero. The  $\pi$ -bond order for the benzyl radical is 0.5 compared to 0.15 for the benzyl-plus-toluene TS structure. Overlap between the reaction site and the phenyl group is definitely attenuated in the benzyl-plus-toluene TS. This analysis shows that reactants will be stabilized more than the TS when a phenyl or other delocalizing group is substituted for methyl in the ethyl-plus-ethane transition structure.

C-H bond distances for H abstraction TSs are presented in Tables 1-3. Consistent with the Hammond-Lefler postulate, the C-H bond distance for the hydrogen being transferred depends on the exothermicity of the reaction: the greater the exothermicity, the shorter is the origin C-H distance and the longer is the terminus C-H distance. Also, the donor moiety becomes slightly more pyramidal while the radical moiety becomes less pyramidal compared to the thermoneutral methyl-plus-methane reaction. For example, in the TS structure for the reaction of methyl radical with methane, the methyl carbon atom is 0.295 Å from the plane defined by the methyl hydrogens, whereas for the reaction of methyl with isobutane, the carbon atom is 0.247 Å from the plane defined by the methyl hydrogens.

Trends in the geometries calculated by PM3 differ from ab initio results. Yamataka and Nagase<sup>12</sup> calculated the TSs for alkyl radical identity reactions at the UHF MP2/6-31G\*/3-21G level. The C-H bond distances for the inflight H ranged between 1.35 and 1.36 Å. Higher level ab initio calculations find inflight C-H bond distances for ethyl-plus-ethane and methyl-plus-methane to be 1.326 Å<sup>7</sup> and 1.323 Å,<sup>37,38</sup> respectively. PM3 calculates the distances to differ significantly according to the degree of branching (see Table 2 or 3),

(37) Calculation was performed by J. A. Franz in the same way as the calculation for ethyl-plus-ethane.<sup>7</sup>

increasing in length according to the series methyl-plus-methyl (1.275 Å) < ethyl-plus-ethane (1.308 Å) < isopropyl-plus-propane (1.340 Å) < *tert*-butyl-plus-butane (1.369 Å).

**Barriers for H Abstraction Identity Reactions.** Table 3 shows results for alkyl and  $\pi$ -conjugated radicals attacking their hydrocarbon precursors. Barriers obtained from both uncorrected and corrected TSs are listed as  $E_a$  and  $E_a'$ , respectively. While few of the barriers in Table 3 have been measured experimentally, the correction tends to give values that are more acceptable, raising low values and reducing large ones (e.g.,  $E_a = 1$  kcal/mol for reactions of isopropyl and *tert*-butyl radicals and  $E_a = 28.7$  kcal/mol for diphenylmethyl). Experimental values for methyl, benzyl, and diphenylmethyl are well reproduced by the correction. Trends are modified but not inverted by the corrections.

For the common saturated alkyl/alkane systems, intrinsic barriers for H abstractions decrease in the order methyl > ethyl  $\approx$  *tert*-butyl > isopropyl.<sup>39</sup> Ab initio calculations and valence-bond curve-crossing models<sup>12</sup> predict the order methyl > ethyl > isopropyl > *tert*-butyl. We think that the PM3 result for the *tert*-butyl system is anomalous because PM3 overcompensates for methyl group repulsions that develop in the pyramidal TS. Support for this explanation is found in comparisons of the calculated and experimental energies for the isomeric alicyclic butanes and pentanes.<sup>21</sup> The calculated  $\Delta H_f^\circ$  for *n*-butane is 1.3 kcal/mol larger than the experimental values, whereas isobutane is larger by 2.9 kcal/mol. For the pentanes, the calculated  $\Delta H_f^\circ$  values are larger by 0.6 kcal/mol for *n*-pentane, 2.4 kcal/mol for isopentane, and 4.5 kcal/mol for neopentane. Allowing for this error, the overall trend in alkyl radical H abstraction identity barriers is in keeping with experiment<sup>40</sup> and higher level theory.<sup>12</sup> The downward trend in intrinsic barriers with methyl group substitution shows that branching at the reaction site stabilizes the TS *more* than the reactants.

The results for delocalized radicals show that increasing the degree of conjugation with the reaction site tends to raise activation barriers. This effect was noted by Stein and co-workers<sup>41</sup> who compared the reactivity of methyl, benzyl, and diphenylmethyl radicals. Our calculations for these and other delocalized systems concur with this trend (see Tables 1 and 3). Figure 4 shows that barriers calculated for identity reactions of homologous polyenyl and arylmethyl radicals increase linearly with decreasing R–H bond dissociation energy (BDE). The BDEs decrease because R• is stabilized more than R–H by  $\pi$ -delocalization. The trend shows that reactants, especially radicals, must be stabilized *more* than the TS by  $\pi$ -delocalization. The result is entirely consistent with the calculated structures which show significantly less  $\pi$ -overlap with the breaking/forming C–H bond in the transition structure (see above).

Interestingly, cyclic donors are calculated to have lower intrinsic barriers than acyclic polyenyl and arylmethyl systems. In Table 3, cyclohexadienyl-plus-cyclohexadiene and hydroanthryl-plus-dihydroanthracene systems have substantially lower barriers than their corresponding acyclic systems 1,4-pentadien-

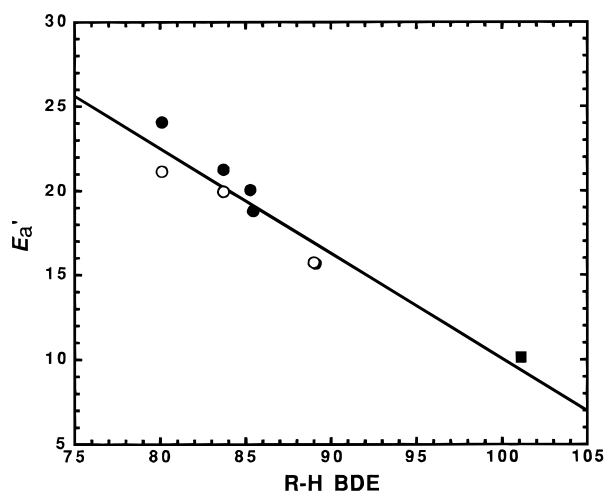
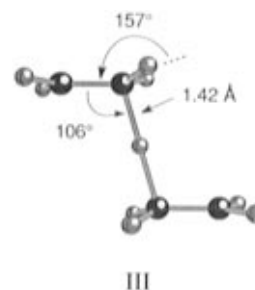


**Figure 4.** Calculated barriers (Table 2) for H abstraction identity reactions of delocalized radicals decrease with increasing donor BDE. This trend shows that  $\pi$ -delocalizing groups stabilize the radical more than the TS. Key: (○) allyl, pentadienyl, heptatrienyl. (●) benzyl, 1-naphthylmethyl, 2-naphthylmethyl, 9-phenanthrylmethyl, 9-anthrylmethyl; (■) ethyl. Units are kilocalories per mole.

3-yl-plus-1,4-pentadiene and diphenylmethyl-plus-diphenylmethane. Cyclic hydroaromatic donors are better than arylalkyl donors for the benzyl radical<sup>29a,b</sup> and for coal liquefaction.<sup>42</sup> Having lower intrinsic barriers for donating H is probably an important contributing factor.

**Transition Structures for RHT Reactions.** Table 4 lists geometric parameters and bond order information for RHT transition structures. The ethyl-plus-ethylene TS structure (III) is depicted below. It is similar to the ab initio TS structure.<sup>7</sup>



Both have linear C–inflight H–C bond angles, planar carbons  $\beta$  to the inflight H, and pyramidal carbons  $\alpha$  to the inflight H. Other structural parameters compare well too.<sup>43</sup>

Higher systems show similar structural features. Pyramidal origin/terminus carbons are intermediate between  $sp^3$  and  $sp^2$  ( $p$ - $\sigma$ -bond order  $\sim 2.4$ ). The  $p$ - $\pi$ -bond orders for the reaction site carbons range from 0.5 to 0.6, indicating that significant  $\pi$ -bonding between the breaking/forming C–H and adjacent  $p$ -orbitals exists in the thermoneutral RHT transition states. The distances for the breaking/forming C–H bonds in RHT TSs, ranging from 1.4 to 1.5 Å, are longer than ones in the H abstraction TSs. The distance varies inversely with the strength of the precursor C–H bond in the radical. Bond angles also increase with bond strengths. The changes correlate with increases in  $p$ - $\sigma$ -bond order and decreases in  $p$ - $\pi$ -bond order. These trends indicate that the radical-like character of the TS is directly related to the strength of the hydroaryl radical  $\beta$ -C–H bond.

(42) Bedell, M. W.; Curtis, C. W. *Energy Fuels* **1991**, 5, 469–476.

(43) Reaction site parameters (parameter, ab initio value,<sup>7</sup> PM3 value):  $C_\alpha$ -H $^\ddagger$ , 1.357 Å, 1.424 Å;  $C_\beta$ - $C_\alpha$ -H $^\ddagger$ , 112.8°, 106.2°;  $H_{\beta 1}$ - $C_\alpha$ - $H_{\beta 2}$ , 113.4°, 113.3°;  $H_\beta$ - $C_\alpha$ -H $^\ddagger$ , 95.2°, 94.1°.

(38) Also see the following calculations: (a) Leroy, G.; Sana, M.; Tinant, A. *Can. J. Chem.* **1985**, 63, 1447. (b) Wildman, T. A. *Chem. Phys. Lett.* **1986**, 126, 325–329. (c) Litwinowicz, J. A.; Ewing, D. W.; Jurisevic, S.; Manka, M. J. *J. Phys. Chem.* **1995**, 99, 9709–9716.

(39) If the barriers are obtained by using uncorrected PM3 energies for the reactants, then an opposite and erroneous trend is obtained (kcal/mol): methyl, 11.7; ethyl, 13.5; isopropyl, 14.7; *tert*-butyl, 18.6.

(40) Identity barriers for *tert*-butyl and isopropyl radicals are estimated to be approximately 11 kcal/mol from experimental data<sup>17</sup> for the cross-reactions of isobutane and propane with methyl and ethyl radicals.

(41) Manka, M. J.; Brown, R. L.; Stein, S. E. *Int. J. Chem. Kinet.* **1987**, 19, 943–957.

**Table 4.** Barriers Calculated for RHT Identity Reactions

no.	RHT identity reaction	C···H <sup>‡</sup> dist (Å)	$\Delta H_f^\circ$ (kcal/mol) <sup>a</sup>				$E_a$	$E_a'^b$	$E_a''^b$	BDE(AH <sup>•</sup> )
			TS	AH <sup>•</sup>	A					
1	ethylene-plus-ethyl	1.420	67.6 (73.6)	28.85	12.5	26.8	25.6	27.2	35.8	
2	butadiene-plus-2-butenyl	1.401	91.6 (95)	31.7	26.1 <sup>c</sup>	34.4	30.2	32.8	46.5	
3	hexatriene-plus-2,4-hexadienyl	1.401	119	39.5 <sup>d</sup>	40	40	32.4	35.6	52.6	
4	benzene-plus-cyclohexadienyl	1.469	90.3 (94.1)	49.7 <sup>e</sup>	19.8	21.4	17.3	19.9	22.2	
5	naphthalene-plus-1-hydronaphthyl	1.453	122.57 (128)	57.1 <sup>e</sup>	35.9	30.2	22.1	25.3	30.9	
6	naphthalene-plus-2-hydronaphthyl	1.461	123.88	59 <sup>e</sup>	35.9	29.1	20.8	24.1	28.5	
7	phenanthrene-plus-9-hydrophenanthryl	1.451	149.77	65.8 <sup>e</sup>	49.7	34.9	23.4	27.1	36	
8	pyrene-plus-1-hydropyrenyl	1.443	167	70 <sup>e</sup>	58.3 <sup>f</sup>	39.7	26	30.1	40.4	
9	anthracene-plus-9-hydroanthryl	1.441	157.00 (167)	64 <sup>e</sup>	55	38.6	26.2	30.1	43.1	
10	propene-plus-1-propyl	1.413	52.9	24	4.8	24.7	25.3	27.2	32.9	
11	propene-plus-2-propyl	1.460	45.1	21.5	4.8	19.4	21	22.7	35.4	
12	isobutene-plus-isobutyl	1.490	39.6	16.8	−4	27.4	29.7	31.3	31.3	
13	2-butene-plus-2-butyl	1.452	28.9	16	−2.9	16.4	20	21.4	33.2	
14	isobutene-plus- <i>tert</i> -butyl	1.406	22.06	12.2	−4	14.5	18.9	20.2	35.9	
15	2,4-dimethyl-2-butene-plus-2,4-dimethyl-2-butyl	1.476	−0.4	2.2	−16.6	14.6	21.9	22.7	33.3	
16	toluene-plus-6-methylcyclohexadienyl	1.500	78.37	42.6 <sup>g</sup>	12	24.4	21.6	24.2	21.5	
17	toluene-plus-3-methylcyclohexadienyl	1.465	71.18	40.4 <sup>h</sup>	12	19.4	17.5	23.3	23.7	

<sup>a</sup> Experimental  $\Delta H_f^\circ$  for hydrogen acceptors (A) and hydrogen donors (AH<sup>•</sup>) obtained from ref 30 or ref 21, unless noted; values in parentheses are AM1 calculations. <sup>b</sup>  $E_a'$  obtained by scaling the calculated TS energy using  $\Delta H_{f,real}^\circ = 0.87\Delta H_{f,calcd}^\circ + 7.1$  kcal/mol from eq 6;  $E_a''$  obtained using  $\Delta H_{f,real}^\circ = 0.89\Delta H_{f,calcd}^\circ + 8.1$  kcal/mol from eq 7. <sup>c</sup> Reference 22. <sup>d</sup> Assumes  $\Delta H_f^\circ = \Delta H_f^\circ(\text{pentadienyl}) + \Delta H_f^\circ(\text{2-butenyl}) - \Delta H_f^\circ(\text{allyl})$ . <sup>e</sup> Reference 61. <sup>f</sup> Estimated from AM1 and PM3 correlations of calculated  $\Delta H_f^\circ$  vs experimental  $\Delta H_f^\circ$ . <sup>g</sup> Assumes  $\Delta H_f^\circ = \Delta H_f^\circ(\text{cyclohexadienyl}) + [\Delta H_f^\circ(\text{isobutane}) - \Delta H_f^\circ(\text{propane})]$ . <sup>h</sup> Assumes  $\Delta H_f^\circ = \Delta H_f^\circ(\text{cyclohexadienyl}) + [\Delta H_f^\circ(\text{tert-butyl}) - \Delta H_f^\circ(\text{isopropyl})]$ .

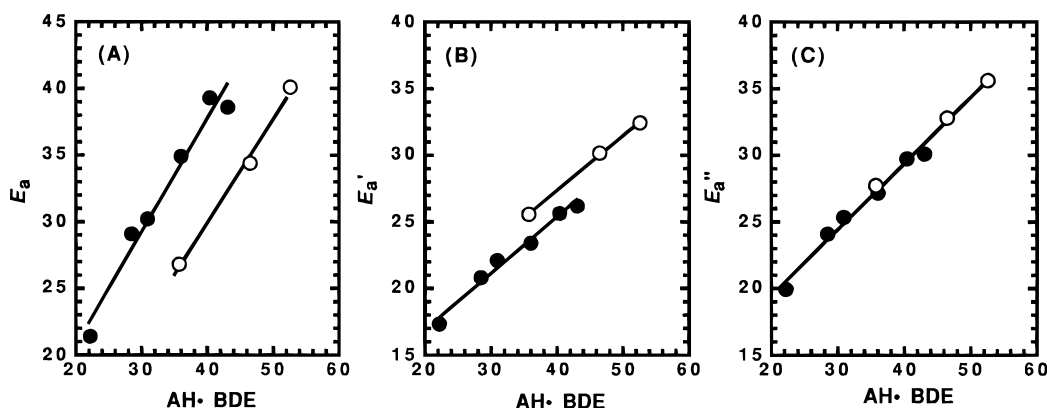


**Figure 5.** Calculated/corrected barriers for RHT identity reactions of delocalized radicals increase with the radical  $\beta$ -C–H BDE: (○) ethyl, 2-butenyl, 2,4-hexadienyl; (●) cyclohexadienyl, 1-hydronaphthyl, 2-hydronaphthyl, 9-hydrophenanthryl, 1-hydropyrenyl, 9-hydroanthryl. (A)  $E_a$  calculated using PM3 TS energies (Table 4). (B)  $E_a'$  obtained by correcting the PM3 (RHT) TS energies with scaling factors derived for H abstraction TS energies (assumes eq 6 is applicable to RHT reactions). (C)  $E_a''$  obtained by correcting PM3 (RHT) TS energies using eq 7, which was optimized to make arene and polyene systems fit the same trend and reproduce the ab initio barrier for ethyl-plus-ethylene RHT. Units are kilocalories per mole.

**Barriers for RHT Identity Reactions.** Calculations of TS energies for ethyl-plus-ethylene and higher homologs were performed to elucidate structure–reactivity trends for the RHT reaction. Table 4 lists data and results of calculations on the RHT reactions that were studied. Effects of conjugation in alicyclic and cyclic (arene) systems (entries 1–9) and of methyl group substitution were examined (entries 11–17). Three  $E_a$  values are listed for each entry in Table 4.<sup>44</sup> One set corresponds to the barriers calculated using PM3 TS energies. The other two are calculated using corrected PM3 TS energies. The rationale for making corrections is discussed below. Table 4 also lists BDEs (AH<sup>•</sup> → A + H<sup>•</sup>) for the radical  $\beta$ -C–H bond that is broken/formed in the RHT reactions. Results for delocalized systems are described first. Then, results for methyl homology of ethyl-plus-ethylene and cyclohexadienyl-plus-benzene systems are presented.

The calculated barriers for acyclic delocalized systems increase in the order ethyl-plus-ethylene < 2-butenyl-plus-butadiene < 2,4-hexadienyl-plus-hexatriene (entries 1–3). Bar-

riers for hydroaryl-plus-arene systems (entries 4–9) increase in the order cyclohexadienyl-plus-benzene < 2-hydronaphthyl-plus-naphthalene < 1-hydronaphthyl-plus-naphthalene < 9-hydrophenanthryl-plus-phenanthrene < 1-hydropyrenyl-plus-pyrene < 9-hydroanthryl-plus-anthracene. These trends parallel the  $\beta$ -C–H bond strengths of the donor radicals. For delocalized radicals, the strength of this bond increases with the degree of  $\pi$ -delocalization because the radicals (AH<sup>•</sup>) are stabilized more than the corresponding polyenes/arenes (A) by vinyl/benzo homologies. Similarly, the trend for calculated RHT barriers implies that the reactants, mainly the donor radicals (AH<sup>•</sup>), are stabilized more than the TS by  $\pi$ -delocalization. Good linear correlations are obtained for fits of RHT barriers vs C–H bond strengths of delocalized AH<sup>•</sup> donor radicals (see Figure 5a), indicating that the BDE may be a good indicator of relative RHT barrier heights.

The trend of greater RHT barriers for more delocalized systems is consistent with the effect of delocalization on H abstraction barriers (see Figure 4). Although the trends, H abstraction barriers increasing with the BDE (RH → A + H<sup>•</sup>) of H donor compounds and RHT barriers decreasing with AH<sup>•</sup> BDEs, appear contradictory, both are consistent when the effects

(44) The reactant energies listed in the table and used to calculate  $E_a$  values are either experimentally measured literature values or estimates obtained by making corrections to calculated values as noted in Table 4.

of delocalization are considered. Both the barriers for RHT and H abstraction reactions involving delocalized systems increase with increasing delocalization. The correlations with BDEs go in opposite directions because delocalized radicals are produced in the dissociation of R–H while they are consumed in the dissociation of AH•.

Although the barrier calculated for ethyl-plus-ethylene RHT compares well with the ab initio barrier,<sup>7</sup> the other uncorrected RHT barriers probably are not equally accurate. As pointed out above, the arene/polyene-radical character of the RHT TS is calculated to vary with the degree of conjugation in the reactants. Since PM3  $\Delta H_f^\circ$  values of delocalized radicals, arenes, and polyenes have different systematic errors, the accuracy of RHT TS energies probably will vary with the mix of radical-arene/polyene character in the TS. The following analyses of  $E_a$  values for delocalized systems support this assertion.

Figure 5 shows the uncorrected barriers plotted against AH• BDE fall into two families, one for cyclic systems and one for acyclic systems. Lines through the uncorrected barriers have similar slopes but are offset by several kilocalories per mole (linear regression parameters: alicyclic, slope  $0.78 \pm 0.06$ , intercept  $1.2 \pm 2.7$  kcal/mol; cyclic, slope  $0.85 \pm 0.08$ , intercept  $3.7 \pm 2.7$  kcal/mol). The intercepts correspond to barriers of hypothetical systems for which AH• BDEs are 0. In such a system, the RHT barrier might approach the barrier of H atom addition. While these barriers are typically only a few kilocalories per mole,<sup>8</sup> thermoneutral reactions could have barriers that are much larger. Therefore, barriers calculated for butadiene and hexatriene systems probably are systematically overestimated.<sup>45</sup>

The barriers for hydroaryl/arene systems are also suspect. Although the regression line has a positive nonzero intercept, the slope of the line is greater than the slope for alicyclic systems, such that calculated barriers are about as great as hydroaryl AH• BDEs. Yet, PM3 TS energies are substantially less than the combined PM3 energies for a H atom and two arenes.<sup>46</sup> This inconsistency suggests that TS energies are overestimated by PM3 and probably need correcting.

Due to a lack of rate data for hydrocarbon RHT reactions, calculated TS energies cannot be correlated with experimental values to correct the TS energies. Therefore, correction factors have been estimated by two different methods which give rise to corrected RHT barriers,  $E_a'$  and  $E_a''$  in Table 4. These corrections tend to reduce the intrinsic barriers for RHT reactions involving delocalized systems. However, the general trend of increasing barrier with increasing delocalization is preserved.

The first approach assumes the correlation obtained for H abstraction TS energies also applies to RHT TS energies. Accordingly, eq 6 is used to generate corrected RHT TS energies that are then used to calculate  $E_a'$ . Figure 5b shows that correction of TS energies with eq 6 leads to barriers for cyclic and acyclic systems that are nearly accommodated by a single correlation. Lines through the two families have slopes of 0.42 (arenes) and 0.41 (alicyclic polyenes) and are offset by 2.7 kcal/mol. The magnitudes of these intercepts, 8.3 kcal/mol for arene systems and 11 kcal/mol for polyene systems, are consistent

with the above arguments that these values should be comparable to the activation barriers for thermoneutral H atom addition reactions.

The second approach, which generates the barrier  $E_a''$  assumes (1) a linear correlation analogous to eq 6 can relate calculated RHT TS energies to real ones, (2) the barrier for ethyl-plus-ethylene equals the ab initio value, 27.2 kcal/mol,<sup>7</sup> and (3) RHT barriers for polyene and arene systems exhibit a single linear correlation with AH• BDEs (see Figure 5c). These conditions yield eq 7, which relates calculated TS to “real” TS energies. It

$$\Delta H_{f,\text{calcd}}^\circ(\text{TS}) = 1.12\Delta H_{f,\text{real}}^\circ(\text{TS}) - 9.02 \text{ kcal/mol} \quad (7)$$

was obtained by adjusting the slope and intercept to maximize the correlation coefficient ( $r^2$ ) of the line in Figure 5c which plots  $E_a''$  vs AH• BDEs for delocalized systems. The resulting line has a slope of 0.5 and an intercept of 9 kcal/mol. Using eq 7 instead of eq 6 to correct RH TS energies causes  $E_a''$  to be greater than  $E_a'$  by approximately 2–4 kcal/mol.

The effects of adding two, four, six, and eight methyl groups to the ethyl-plus-ethylene system were examined by calculating the barriers for propyl-plus-propene, isopropyl-plus-propene, *sec*-butyl-plus-*trans*-2-butene, *tert*-butyl-plus-isobutene, and 2,3-dimethyl-2-butyl-plus-2,3-dimethyl-2-butene. The barriers are listed in Table 4, entries 10–15. While the corrections tended to raise the barriers of these systems, neither corrected nor uncorrected barriers correlate with alkyl radical  $\beta$ -C–H BDEs. Although, a general trend is apparent: methyl group substitutions at the radical site lower the barrier while substitutions at  $\beta$ -positions from which the H originates raise the barrier. For example, 2-propyl-plus-propene < 1-propyl-plus-propene, *tert*-butyl-plus-isobutene < 2-butyl-plus-isobutene < isobutyl-plus-isobutene, 2,3-dimethyl-2-butyl-plus-2,3-dimethylbutene < isobutyl-plus-isobutene.

The effect of methyl substitutions on the cyclohexadienyl-plus-benzene system was also explored. Barriers for RHT reactions of two isomeric toluene-based systems were calculated. In one system (entry 16, Table 4), the methyl group is *ipso* to the reaction site; in the other system entry 17, Table 4), the methyl is *para* to the reaction site. The barriers for these reactions are larger than the barrier for transfer from cyclohexadienyl to benzene, consistent with their C–H bonds being stronger than the C–H in the cyclohexadienyl radical. *Ipso* substitution increased the barrier relatively more than *para* substitution, even though the C–H in the 6-methylcyclohexadienyl radical is weaker than the C–H in the 3-methylcyclohexadienyl radical. This effect is analogous to the effect observed for methyl substitution of the ethyl-plus-ethylene system: substitution  $\beta$  to the radical site raises the barrier.

## Discussion

The above results show that H transfer barriers calculated using suitably-corrected MNDO-PM3 TS energies provide reliable qualitative, if not quantitative, structure–barrier trends. The results are well supported by both experiment and ab initio calculations on prototypical systems. While no measurement of an RHT barrier is available to gauge the accuracy of the ab initio result for ethyl-plus-ethylene, the ab initio method was found to reproduce the AH• BDE of the ethyl radical<sup>7</sup> and give satisfying agreement for the H abstraction barriers of ethyl-plus-ethane<sup>7</sup> and methyl-plus-methane<sup>47</sup> reactions (15.5 and 17.7 kcal/mol, respectively, vs experimental values of 13.3 and 14.6

(45) Note that PM3  $\Delta H_f^\circ$  values for arenes and polyenes are greater than experimental values and the difference increases with molecular size. Since the RHT TS may be viewed as a H atom in transition between two arene-like moieties, errors in  $\Delta H_f^\circ$  for RHT TSs may similarly increase with molecular size.

(46) Using PM3 energies for the RHT TS and corresponding arene, dissociation of the TS,  $[\text{A}\cdots\text{H}\cdots\text{A}]^\ddagger \rightarrow 2\text{A} + \text{H}^\bullet$ , is calculated to be endothermic for the hydroaryl/arene systems (AH• in  $[\text{A}\cdots\text{H}\cdots\text{A}]^\ddagger$ ,  $\Delta H$  (kcal/mol)): cyclohexadienyl, 8; 1-hydronaphthyl, 11; 9-hydrophenanthryl, 12; 9-hydroanthryl, 18.

(47) The same type of ab initio calculation as described in ref 7 for the ethyl-plus-ethane reaction (structure, energy (hartrees)): methyl radical, –39.665 54; methane, –40.320 39; methyl-plus-methane TS, –79.9577.



kcal/mol), considering that tunneling effects tend to cause measured barriers to be lower than adiabatic barriers.<sup>17,38,48,49</sup> Therefore, the ab initio and PM3 barriers for ethyl-plus-ethylene RHT are considered to be representative of the experimental barrier. The RHT barriers estimated for higher systems are admittedly uncertain. However, the structure–barrier trends are expected to be qualitatively correct, for they parallel analogous trends that have been calculated and experimentally verified for H abstraction reactions.

The findings clearly indicate that the RHT reaction is intrinsically more difficult than H abstraction. Depending on the structures involved, intrinsic barriers for hydrocarbon RHT reactions may range from 60% to 90% of the  $\beta$ -C–H bond energy. In contrast, H abstraction reactions occur with barriers that are a small fraction ( $\sim 15\%$  for ethyl-plus-ethane) of the donor C–H bond energy.

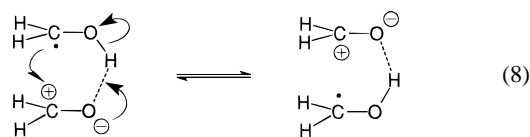
Inspection of the TS geometries calculated for H abstraction and RHT reactions provides fundamental insights to both the noted effects of  $\pi$ -delocalizing groups and the substantial difference between H abstraction and RHT barriers. TS structures for H abstraction resemble a H atom in transit between two alkyl groups, not alkyl radicals. Frequencies for pyramidal distortion of methyl, ethyl, isopropyl, and *tert*-butyl radicals are 605, 540, 382, and  $<200$   $\text{cm}^{-1}$ .<sup>50</sup> In comparison, methyl, methylene, and methine group symmetric angle deformations have frequencies corresponding to 1378, 1463, and 1350–1315  $\text{cm}^{-1}$ .<sup>51</sup> Thus, radical  $\text{sp}^2$  carbons exhibit lower barriers to pyramidal distortion compared to that for planar distortion of alkyl  $\text{sp}^3$  carbons. Consequently, much of the structural reorganization occurs at the radical carbon. Overlap with adjacent  $\pi$ -delocalizing groups is diminished in the TS such that the reactants are stabilized more than the TS by  $\pi$ -delocalization, with the net result being larger barriers for more delocalized (but otherwise homologous) systems. For the RHT reaction, the radical site is remote to the reaction site and does not distort from planarity. Carbons with greater reorganization energies,  $\text{sp}^3$  alkyl and  $\text{sp}^2$  alkene/arene,<sup>52</sup> are at the reaction site and must deform to achieve the TS geometry. The  $\text{sp}^3$  carbon that is donating the H atom deforms substantially toward  $\text{sp}^2$  character to achieve the TS. With these insights, the greater barriers for RHT compared to H abstraction are not surprising. The increase in barrier with benzannulation of the cyclohexadienyl-plus-benzene system and vinylogous homologation of the ethyl-plus-ethylene system is also consistent with these insights. The loss of radical character and development of olefin/arene character on forming the RHT TS causes the reactants to derive more stabilization from the homologations than the TS does. Similarly, the stabilities of  $\text{AH}^\bullet$  radicals increase more than the stabilities of olefins or arenes from vinyl or benzo homologations, which explains why RHT barriers may correlate with the  $\text{AH}^\bullet$  BDEs.

Another example of conjugation effects acting to stabilize reactants more than the TS because of decreased  $\pi$ -overlap in the TS has been discussed in the recent literature. Héberger, Walbiner, and Fischer<sup>53</sup> measured rate constants for *para*-

substituted benzyl radicals adding to a variety of *gem*-substituted alkenes. They found “no obvious correlation with radical singly occupied molecular orbital energies nor with  $\sigma$  scales for benzyl substituents”, and suggested that the low *para*-substituent effects may be due to a decrease in mesomeric and inductive effects caused by deformation of the benzylic radical in the TS.

For the RHT reaction to play a role in condensed phase hydrocarbon pyrolyses, barriers need to be substantially less than the barriers for formation of free H atoms and for reverse radical disproportionation. Autrey et al.<sup>54</sup> recently used a mechanistic kinetic modeling approach to estimate maximum RHT barriers necessary to contribute to solvent-induced scissioning of strong alkyl aromatic bonds by mixtures of aromatic and hydroaromatic solvents. They found that intrinsic RHT barriers needed to be  $\leq 14$  kcal/mol for benzene systems,  $\leq 17$  kcal/mol for anthracene systems, and  $\leq 19$  kcal/mol for phenanthrene systems. These barriers are smaller than our estimates of the RHT barriers by a margin sufficient to raise doubt about the occurrence of RHT reactions in hydrocarbon pyrolyses, especially the thermoneutral or endothermic cases.

In contrast to hydrocarbon systems, the barrier for RHT between ketyl radicals and ketones is surprisingly facile. Rate constants for room temperature reactions range as large as  $10^3$ – $10^4$   $\text{M}^{-1} \text{s}^{-1}$ .<sup>6a</sup> Ketyl/ketone RHT reactions seem to be fundamentally different from those of hydrocarbon systems. Naguib et al.<sup>6b</sup> postulate that the reaction proceeds from the H-bonded complex via electron transfer concerted with proton transfer (eq 8). Theoretical calculations (PMP2/6-31G\*\*) performed in this laboratory appear consistent with this view and will be reported in a separate paper.



## Conclusions

These calculations clearly show that symmetric barriers for H transfer are dependent on the structures of the radicals. The variation in these intrinsic barriers is greater in degree and of a fashion not well appreciated by the research community. These facts, together with uncertainties caused by the tunnel effect,<sup>48,49,55</sup> provide impetus for measuring H transfer rates. Also, this study further elucidates how bond reorganization (bond stretching and angle deformation) contributes to H transfer barriers. Pross et al.<sup>13</sup> have used a qualitative valence-bond curve-crossing model to explain structure–reactivity trends for H abstraction reactions of saturated hydrocarbons.<sup>56</sup> The model explains the decrease in intrinsic barriers for alkyl radicals with increased branching by correlating the crossing point of ground and excited state surfaces with alkane BDEs. However, this correlation with BDEs does not extend to conjugated systems because radical site angle deformations in the TS offset

(54) Autrey, T.; Alborn, E. A.; Franz, J. A.; Camaioni, D. M. *Energy Fuels* **1995**, *9*, 420–428.

(55) Truhlar, D. G.; Gordon, M. S. *Science* **1990**, *249*, 491. Garrett, B. C.; Joseph, T.; Truong, T. N.; Truhlar, D. G. *Chem. Phys.* **1989**, *136*, 271–283. Garrett, B. C.; Truhlar, D. G.; Wagner, A. F.; Dunning, T. H., Jr. *J. Chem. Phys.* **1983**, *78*, 4400–4413. Garrett, B. C.; Koszykowski, M. L.; Melius, C. F.; Page, M. *J. Phys. Chem.* **1990**, *94*, 7096–7106.

(56) For examples of the application of curve-crossing models to radical addition to olefins, see: Wong, M. W.; Pross, A.; Radom, L. *Isr. J. Chem.* **1994**, *33*, 415–25; *J. Am. Chem. Soc.* **1994**, *116*, 6284–6292, 11938–11943.

(57) (a) Ingold, K. U. In *Free Radicals*; Kochi, J. K., Ed.; Wiley: New York, 1973; Vol. 1, pp 74, 75.

(58) Stein, S. E.; Brown, R. L. *J. Am. Chem. Soc.* **1991**, *113*, 787–793.

(48) Trotman-Dickenson, A. F. *Adv. Free Radical Chem.* **1965**, *1*, 1.

(49) Bell, R. P. *The Tunnel Effect in Chemistry*; Chapman and Hall: New York, 1980; pp 106–140.

(50) Pacansky, J.; Koch, W.; Miller, M. D. *J. Am. Chem. Soc.* **1991**, *113*, 317–328.

(51) Colthup, N. B.; Daly, L. H.; Wiberley, S. E. *Introduction to Infrared and Raman Spectroscopy*, 3rd ed.; Academic Press, Inc.: San Diego, CA, pp 215–233.

(52) Out-of-plane (hydrogen wag) vibrational frequencies for vinyl and vinylidene  $\text{CH}_2$  groups are 910–905 and 895–885  $\text{cm}^{-1}$ . See ref 51, pp 248, 250, and 252.

(53) Héberger, K.; Walbiner, M.; Fischer, H. *Angew. Chem., Int. Ed. Engl.* **1992**, *31*, 635–636.

resonance stabilization energies. Such insight cannot be discerned from qualitative curve-crossing models.

With respect to the RHT reaction, these findings necessitate a reassessment of the postulated role of RHT in high-temperature reactions of aromatic hydrocarbons. The barrier may be much higher than originally postulated.<sup>4</sup>

Finally, although PM3 and AM1 values for H abstraction TSS

(59) PM3  $\Delta H_f^\circ$  values are for the following methylarenes (kcal/mol): 1-methylnaphthalene, 32.59; 2-methylnaphthalene, 31.44; 9-methylphenanthrene, 47.10; 9-methylanthracene, 54.30. Correcting these respective values downward by 4.79, 4.84, 6, and 6.7 kcal/mol, the differences between the PM3 and experimental values for the parent arenes,<sup>21</sup> yields values of 27.8, 26.6, 41.10, and 47.60 kcal/mol for the respective compounds. The experimental values for 1- and 2-methylnaphthalenes are  $27 \pm 0.5$  kcal/mol. Lias et al.<sup>21</sup> estimate the values for 9-methylphenanthrene and 9-methylanthracene as 42 and 48 kcal/mol.

(60) (a) Experimental values for these radicals estimated by assuming  $\Delta H_{f,\text{exptl}}^\circ(2\text{-naphthylmethyl}) = \Delta H_{f,\text{exptl}}^\circ(1\text{-naphthylmethyl}) + \Delta H_{f,\text{PM3}}^\circ(2\text{-naphthylmethyl}) - \Delta H_{f,\text{PM3}}^\circ(1\text{-naphthylmethyl})$  and  $\Delta H_{f,\text{exptl}}^\circ(9\text{-phenanthrylmethyl}) = \Delta H_{f,\text{exptl}}^\circ(9\text{-anthrylmethyl}) + \Delta H_{f,\text{PM3}}^\circ(\text{phenanthrylmethyl}) - \Delta H_{f,\text{PM3}}^\circ(9\text{-anthrylmethyl})$ . The PM3  $\Delta H_f^\circ$  values calculated for 1- and 2-naphthylmethyl, 9-anthrylmethyl, and 9-phenanthrylmethyl are, respectively, 69.6, 70.2, 85.5, and 84.1 kcal/mol. Plugging the PM3 values into the correlation ( $r^2 = 0.995$ ) of PM3 vs experiment<sup>35</sup> for allyl, pentadienyl, benzyl, and 9-anthrylmethyl yields the same value for 9-phenanthrylmethyl, but different values for 1- and 2-naphthylmethyl: 63.4 and 63.8 kcal/mol, respectively. (b) The estimate for  $\Delta H_f^\circ$  of heptatrienyl was obtained by substituting the PM3 value (65.1 kcal/mol) into the above correlation.

differ, they both correlate linearly with experimental values. Thus, studies using either MNDO-PM3 or AM1 arrive at the same conclusions, provided that the appropriate corrections are made.

**Acknowledgment.** This work was supported by the U.S. Department of Energy, Office of Basic Energy Research, Division of Chemical Sciences, Processes and Techniques Branch. The authors thank Dr. Kim F. Ferris (PNL) for discussions. We gratefully acknowledge the support for T.B.S. through DOE's Undergraduate Summer Research Student programs (administered in 1993 by the Northwest Association of Colleges and Universities for Science and in 1994–95 by Associated Western Universities-Northwest). The Pacific Northwest National Laboratory is operated for the U.S. Department of Energy by Battelle Memorial Institute under Contract No. DE-AC06-76RLO 1830.

JA950740L

(61) Experimental  $\Delta H_f^\circ$  values for cyclohexadienyl<sup>126</sup> and 9-hydroanthryl<sup>123a</sup> are, respectively, 49.7 and 64 kcal/mol. Estimates for the other hydroaryl radicals assume a linear correlation between PM3 and experimental  $\Delta H_f^\circ$ . PM3  $\Delta H_f^\circ$  (kcal/mol): cyclohexadienyl, 41.3; 1-hydronaphthyl, 53.6; 2-hydronaphthyl, 57.8; 9-hydrophenanthryl, 68.7; 9-hydroanthryl, 65.6; 1-hydroptyrenyl, 76.2.